Diluted Bitumen Water-in-Oil Emulsion Stability and Characterization by Nuclear Magnetic Resonance (NMR) Measurements†

Tianmin Jiang, George Hirasaki,* and Clarence Miller

Department of Chemical Engineering, Rice University, Houston, Texas 77251

Kevin Moran

Syncrude Canada, Ltd., Edmonton Research Centre, 9421 17th Avenue, Edmonton, Alberta T6N 1H4, Canada

Marc Fleury

Institut Français du Petrole (IFP), 1 & 4, Avenue de Bois-Préau, 92852 Rueil−Malmaison Cedex, France

Received September 2, 2006. Revised Manuscript Received April 2, 2007

Canadian oil sands represent a huge oil resource. Stable water-in-oil (W/O) emulsions, which persist in Athabasca oil sands from surface mining, are problematic, because of clay solids. This article focuses on the characterization of water-in-diluted-bitumen emulsions by nuclear magnetic resonance (NMR) measurement and the transient behavior of emulsions undergoing phase separation. An NMR restricted diffusion experiment (pulsed gradient spin−echo (PGSE)) can be used to measure the emulsion drop-size distribution. Experimental data from PGSE measurements show that the emulsion drop size does not change much with time, which suggests that the water-in-diluted-bitumen emulsion is very stable without an added coalescer. The sedimentation rate of emulsion and water droplet sedimentation velocity can be obtained from NMR one-dimensional (1-D) T_1 weighted profile measurement. Emulsion flocculation can be deduced by comparing the sedimentation velocity from experimental data with a modified Stokes' Law prediction. PR_5 (a polyoxyethylene (EO)/polyoxypropylene (PO) alkylphenol formaldehyde resin) is an optimal coalescer at room temperature. For the sample without fine clay solids, complete separation can be obtained; for the sample with solids, a rag layer that contains solids and has intermediate density forms between the clean-oil and free-water layers. Once formed, this rag layer prevents further coalescence and water separation.

1. Introduction

Canadian oil sands represent a huge amount of oil resources. However, oil sands are unconsolidated deposits of very heavy hydrocarbon bitumen and require multiple stages of processing before refining.

Stable water-in-oil (W/O) emulsions, which persist in Athabasca oil sands from surface mining, are problematic, because of clay solids. The stability of the emulsion is very important to the final separation process. The objectives of this study are to show (i) that the time evolution of the stability properties of emulsions can be measured in the laboratory using low-field nuclear magnetic resonance (NMR) techniques and (ii) that the separation of water, oil, and solids can be realized using an appropriate demulsifier in the separation procedure.

2. Materials and Methods

2.1. Materials. Samples of bitumen froth were received from Syncrude Canada, Ltd. The bitumen froth then was diluted with naphtha, at a bitumen/naphtha ratio of 0.42 (w/w). The diluted bitumen contains ∼1% solids and <2% water, which can be measured by centrifugation. Most of the solids and water can be removed by centrifuge process, with a centrifugal acceleration of 3500g and a centrifuge time of 30 min. The aqueous phase used here is 1% (w/w) NaCl brine.

Table 1. Bulk Fluid Properties at 30 °C

bulk fluid	density (g/mL)	viscosity (cP)	$T_{2,peak}$ (s)	diffusivity ($\times 10^{-9}$ m^2/s)
brine	1.001	1.20	2.6	2.6
diluted bitumen	0.815	2.12	0.413	1.0
diluted bitumen after centrifuge	0.814	2.05	0.556	1.3

The bulk fluid properties are listed in Table 1. Here, the viscosities were measured with a Brookfield model DV-III+ rheometer. The T_2 peak value and diffusivity were measured using a MARAN II spectrometer (2.2 MHz, Resonance, Inc.).

2.2. Emulsion Preparation. Emulsion samples (60 mL in volume) were prepared by mixing brine (50 vol %) and diluted bitumen (50 vol %) in a flat-bottom glass tube (outer diameter of 48 mm, inner diameter of 44 mm, and length of 230 mm) with a six-blade turbine (Figure 1). The stirring speed of the turbine was 3600 rpm, and the mixing time was 10 min. Prior to emulsification, the aqueous and oil phases were left in contact in the oven (30 ± 0.1 °C) for 24 h. The prepared emulsion can be used for nuclear magnetic resonance (NMR) measurements.

† Presented at the 7th International Conference on Petroleum Phase Behavior and Fouling.

* Author to whom correspondence should be addressed. Tel.: +1 713 348 5416. E-mail address: gjh@rice.edu.

10.1021/ef0604487 CCC: $37.00
Published on Web 04/27/2007

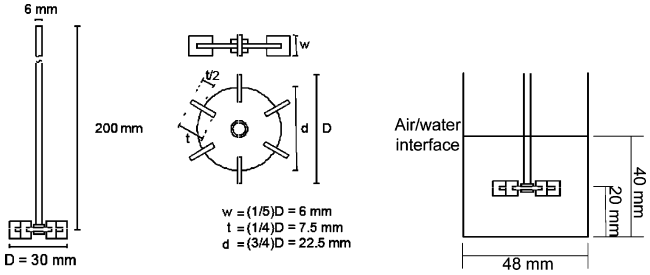

Figure 1. Sketch of the mixer and emulsion preparation.

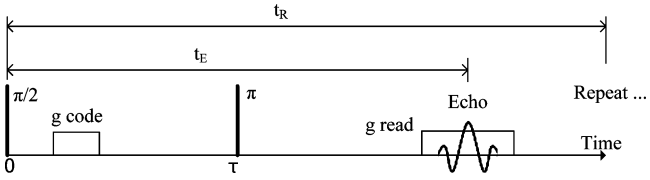

Figure 2. Sequence of one-dimensional (1-D) profile measurement, repeated at time t_R.

2.3. Characterization of Emulsions by NMR. NMR spectroscopy is based on the fact that some nuclei possess a nuclear magnetic moment. NMR is a versatile method for two reasons:[1]

(1) It is a nondestructive technique. The system can be studied without any perturbation that will affect the outcomes of the measurement. The system can be characterized repeatedly with no time-consuming sample preparation between the runs.

(2) A large number of spectroscopic parameters can be determined by NMR, relating to both static and dynamic aspects of a wide variety of systems.

In this study, Carr−Purcell−Meiboom−Gill (CPMG) measurement is used to obtain the T_2 distribution, and restricted diffusion measurement (PGSE) is used to obtain the drop-size distribution of the emulsion.[1] To get volume fraction profiles for different phases, magnetic resonance imaging (MRI) one-dimensional (1-D) profile measurement is used.

In MRI 1-D profile measurement, the sequence consists of a 90° radio-frequency (rf) pulse, followed by a 180° rf pulse at time τ. A spin−echo is collected at time t_E. The 180° rf pulse is between two magnetic-field gradient pulses with strength g, as shown in Figure 2. The magnetic gradient is along the vertical direction z.

A Fourier transform of the spin−echo yields the signal amplitude for each position. The equation of signal amplitude is[2]

$$A = A_0\left[1 - \exp\left(\frac{-t_R}{T_1}\right)\right]\exp\left(\frac{-t_E}{T_2}\right) \quad (1)$$

When the oil/water concentration varies as a function of z, the contrast in the hydrogen index is not large enough to give any information. To generate a contrast based on the relaxation time difference between oil and water, one solution is to perform a T_1 weighted spin density profile. In this case, $t_E \ll T_2$, $\exp(-t_E/T_2) \approx 1$, and the amplitude $A(z)$ at a given position z is given by

$$A(z) = A_\infty\left[1 - \sum \varphi_i(z)\exp\left(\frac{-t_w}{T_{1,i}}\right)\right] \quad (2)$$

Here, φ_i is the volume fraction for component i. A_∞ is the amplitude when t_w is sufficiently long. The parameter t_w represents the waiting time ($t_w = t_R - t_E \approx t_R$); it is chosen to be intermediate between the relaxation times of the oil and the emulsified water, so that different phases can be distinguished. For W/O emulsions, eq 2 can be written as

$$A(z) = A_\infty\left[1 - \varphi_{oil}(z)\exp\left(\frac{-t_w}{T_{1,oil}}\right) - \varphi_{water}(z)\exp\left(\frac{-t_w}{T_{1,water}}\right) - \varphi_{drop}(z)\exp\left(\frac{-t_w}{T_{1,drop}}\right)\right] \quad (3)$$

where the subscripts "oil", "water", and "drop" correspond to continuous oil, bulk water, and water droplets, respectively.

2.4. Selection of Coalescer. Emulsions may degrade via several different mechanisms (for instance, sedimentation/creaming, flocculation, and coalescence). In this study, sedimentation and coalescence were assumed as the primary demulsification mechanisms.

Bottle tests[3] were applied to determine the optimal coalescer for the emulsion sample. Fresh emulsion samples (25 mL in volume) were added to several bottles (outer diameter of 25 mm). Then, 200 ppm of PR_x (polyoxyethylene (EO)/polyoxypropylene (PO) alkylphenol formaldehyde resins with different EO/PO contents; Nalco Energy Services)[3] coalescer solution (50 μL of 10% PR_x xylene solution for the 25-mL emulsion sample) was added to the emulsion samples. Afterward, all the samples were shaken by hand at the same time for 1 min and placed in the oven at 30 °C.

The emulsion sample containing PR_5 had the best separation at room temperature. Thus, in the current study, PR_5 was chosen as the optimal coalescer.

Table 2. Different Emulsion Samples for the Measurement

case	with solids	without solids
without coalescer	sample 1	sample 3
with coalescer	sample 2	sample 4

3. Results and Discussion

The effects of solids and coalescer were investigated using different samples. The four emulsion samples are described in Table 2. The differences between samples 1 and 2 and between samples 3 and 4 show the effects of the coalescer, whereas the differences between samples 1 and 3 and between samples 2 and 4 show the effects of clay solids.

3.1. T_2 Distribution from CPMG Measurement. T_2 distribution evolutions of emulsion samples 1−4 from CPMG measurement are shown in Figures 3−6. In the figures, T_2 distributions of layered oil over water and photographs of the emulsions after 12 h are also shown for reference.

In samples 2 and 4, 200 ppm of PR_5 coalescer solution (120 μL of 10% PR_5 xylene solution for the 60-mL emulsion sample) was added immediately after emulsion preparation. Afterward, all the samples were shaken by hand for 1 min.

Unlike the layered mixture, the T_2 distribution of sample 1 (with solids, no PR_5; see Figure 3) has only one peak. Hence, the water content and drop-size distribution of the emulsion cannot be obtained from CMPG measurement.[1]

The T_2 distribution of sample 2 (with solids and PR_5; see Figure 4) exhibits a larger peak for oil and the W/O emulsion and a smaller peak for the separated bulk water. This is consistent with the observation that free water forms at the bottom of the sample because of the emulsion coalescence (see photograph inset in Figure 4).

The T_2 distributions of sample 3 (no solids, no PR_5; see Figure 5) and sample 4 (no solids, with PR_5; see Figure 6) exhibit

(1) Peña, A. A.; Hirasaki, G. J. Enhanced characterization of oilfield emulsions via NMR diffusion and transverse relaxation experiments. *Adv. Colloid Interface Sci.* **2003**, *105*, 103−150.

(2) Liang, Z.-P.; Lauterbur, P. C. *Principles of Magnetic Resonance*; Akay, M., Ed.; IEEE: New York, 2005; Ch. 7.

(3) Peña, A. A.; Hirasaki, G. J.; Miller, C. A. Chemically Induced Destabilization of Water-in-Crude Oil Emulsions. *Ind. Eng. Chem. Res.* **2005**, *44*, 1139−1149.

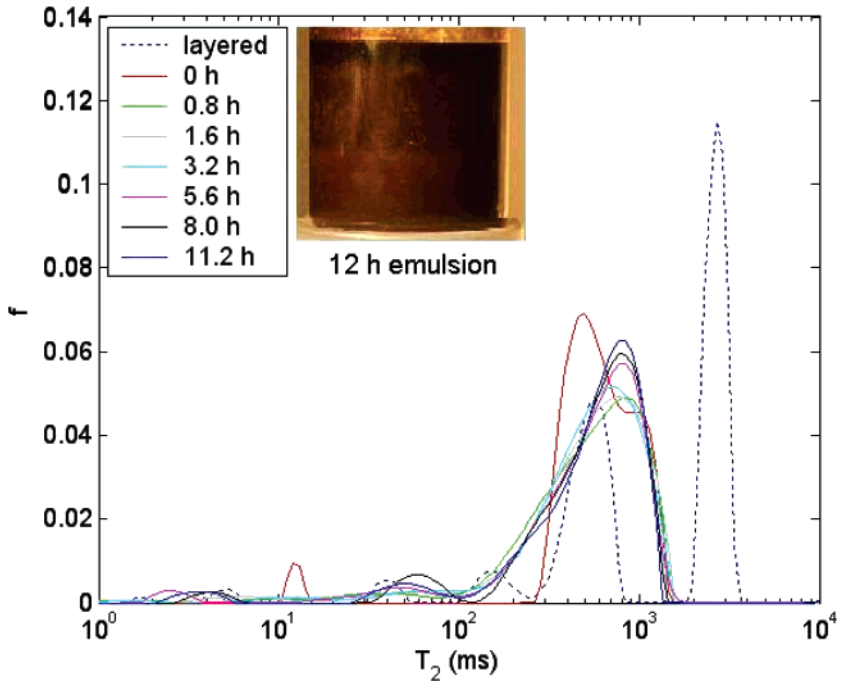

Figure 3. T_2 distribution of emulsion with solids and no PR_5 (sample 1).

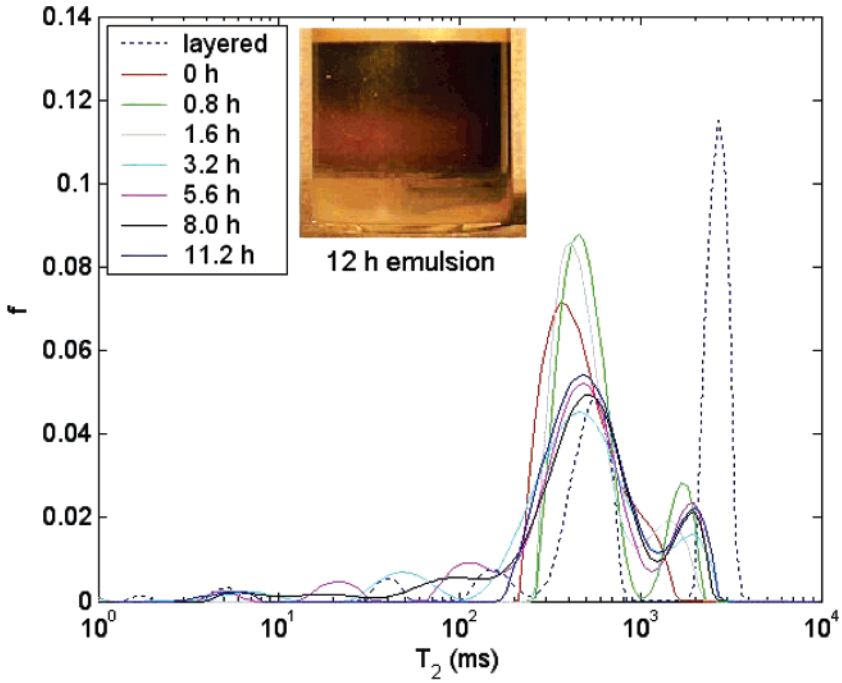

Figure 4. T_2 distribution of emulsion with solids and the addition of PR_5 (sample 2).

two separate peaks, which is different from the two samples with solids. This difference may be due to the effect of the solids.

In sample 3 (no solids, no PR_5; represented by Figure 5), both the oil and water peaks occur at smaller T_2 values than those of the bulk fluids. This shows the effect of surface relaxivity at the W/O interface on the T_2 distribution.

In sample 4 (no solids, with PR_5; represented by Figure 6), the T_2 distribution of the oil peak is very similar to that of bulk oil, and the water peak is similar to that of bulk water, which suggests compete separation of the oil and the water. This is consistent with the visual observations. The T_2 distribution of the water peak is shorter than that of bulk water. From the picture of the emulsion, the water layer is yellowish, which suggests that the water contains some dissolved material, possibly colloidal iron hydroxide, which enhances water relaxation. Thus, the T_2 distribution of the water peak is shorter than that of bulk water.

3.2. Drop-Size Distribution from Restricted Diffusion Measurement. Determination of the drop-size distribution consists of performing a least-squares fit of the experimental signal attenuation (R_{emul}) with different pulse field gradients, using the terms d_{gV}, σ, D_{CP}, and κ as fitting parameters.[1] The fitting results for sample 1 can be observed in Figure 7. Here, κ is the contribution ratio of each component to the total attenuation. A log-normal distribution with mean drop diameter d_{gV} and deviation parameter σ is assumed for the emulsion drop size.

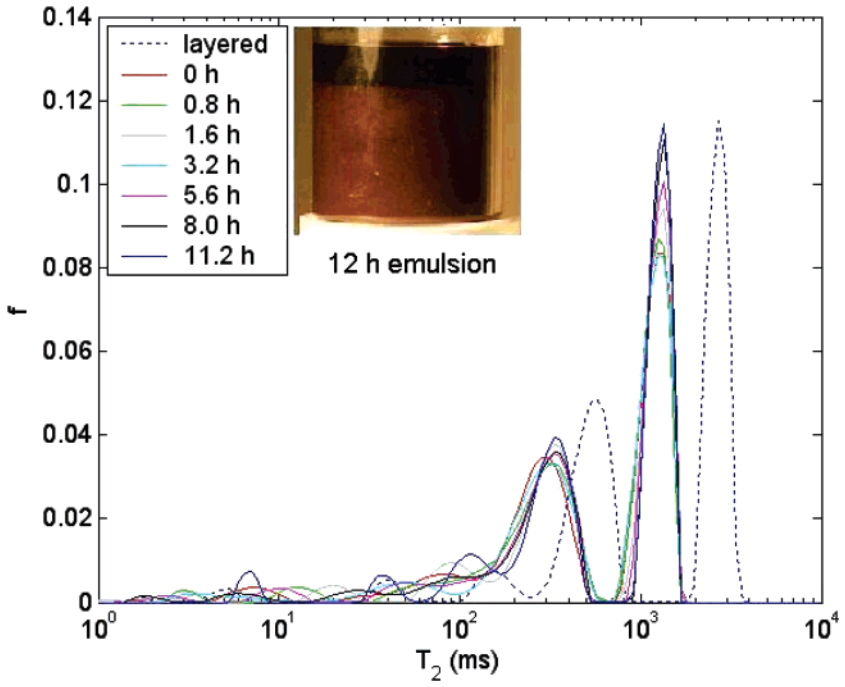

Figure 5. T_2 distribution of emulsion without solids and no PR_5 (sample 3).

For the cases without a coalescer, the emulsion sample contains only oil and emulsified water. The NMR signal attenuation can be expressed as follows:

$$R = \kappa_{oil}R_{oil} + \kappa_{emul}R_{emul} \tag{4a}$$

$$\kappa_{oil} + \kappa_{emul} = 1 \tag{4b}$$

$$\kappa_{oil} = \frac{\sum (f_i)_{oil} \exp[-2\tau/(T_{2,i})_{oil}]}{\sum f_i \exp[-2\tau/(T_{2,i})]} \tag{5a}$$

$$\kappa_{emul} = \frac{\sum (f_i)_{emul} \exp[-2\tau/(T_{2,i})_{emul}]}{\sum f_i \exp[-2\tau/(T_{2,i})]} \tag{5b}$$

Here, the subscripts "oil" and "emul" correspond to continuous oil and emulsified water, respectively. The term f_i represents the fraction of protons with relaxation $T_{2,i}$, and 2τ is the echo spacing in the measurement. κ is the contribution ratio of each component to the total attenuation.

For the cases with added coalescer, emulsion will coalescence and form free water. Thus, in the calculation, eq 4 can be extended as

$$R = \kappa_{oil}R_{oil} + \kappa_{emul}R_{emul} + \kappa_{water}R_{water} \tag{6a}$$

$$\kappa_{oil} + \kappa_{emul} + \kappa_{water} = 1 \tag{6b}$$

$$\kappa_{oil} = \frac{\sum (f_i)_{oil} \exp[-2\tau/(T_{2,i})_{oil}]}{\sum f_i \exp[-2\tau/(T_{2,i})]} \tag{7a}$$

$$\kappa_{emul} = \frac{\sum (f_i)_{emul} \exp[-2\tau/(T_{2,i})_{emul}]}{\sum f_i \exp[-2\tau/(T_{2,i})]} \tag{7b}$$

$$\kappa_{water} = \frac{\sum (f_i)_{water} \exp[-2\tau/(T_{2,i})_{water}]}{\sum f_i \exp[-2\tau/(T_{2,i})]} \tag{7c}$$

where subscripts "oil", "emul", and "water" correspond to the continuous oil phase, dispersed water phase, and separated free-water phase, respectively.

If the NMR diffusion measurement is performed for the emulsion over time, the evolution of the drop-size distribution can be obtained from the fitting calculation of diffusion results.

The time-dependent drop-size distributions of different emulsion samples obtained from diffusion results are shown in Tables 3−6.

In sample 4 (Table 6), after 3.2 h, the diffusion attenuation is <0.01, which implies complete separation of the oil and the water. Thus, in this case, a drop-size distribution of the emulsion cannot be obtained. Here, only the first three results are listed.

From Tables 3 and 5 (for samples 1 and 3), the mean drop diameter, deviation parameter σ, κ_{oil}, and κ_{emul} do not change much with time, which suggests that the emulsion is stable; the κ_{water} values are very low, which shows that coalescence is very slow in the absence of a coalescer (PR_5). In contrast, in Tables 4 and 6 (for samples 2 and 4), κ_{water} increases over time, which demonstrates that the coalescer (PR_5) accelerates the emulsion coalescence. The parameter κ_{emul} in Table 6 (for sample 4) is much smaller than that in Table 4 (for sample 2), which indicates a lower emulsion content. Sample 2 has much more solids than sample 4; thus, the effect of solids is to make the emulsion more stable.

3.3. Phase-Fraction Profile from One-Dimensional (1-D) T_1 Weighted Profile Measurement. NMR 1-D T_1 weighted profile measurement is based on the T_1 difference of different components. Figure 8 shows the profile measurement results of the four emulsion samples in Table 2. The waiting time is t_w = 0.6 s. The imaging pulse field gradient is 0.8 G/cm. In Figure 8, the *x*-axis is the spin−echo signal amplitude of the sample (*A*), and the *y*-axis position is the position measured from the

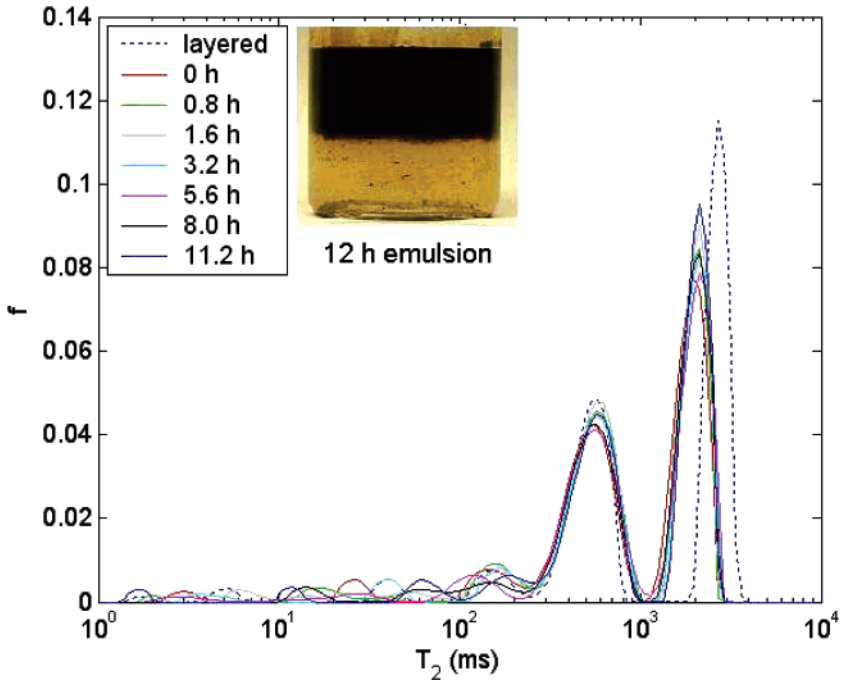

Figure 6. T_2 distribution of emulsion without solids and the addition of PR_5 (sample 4).

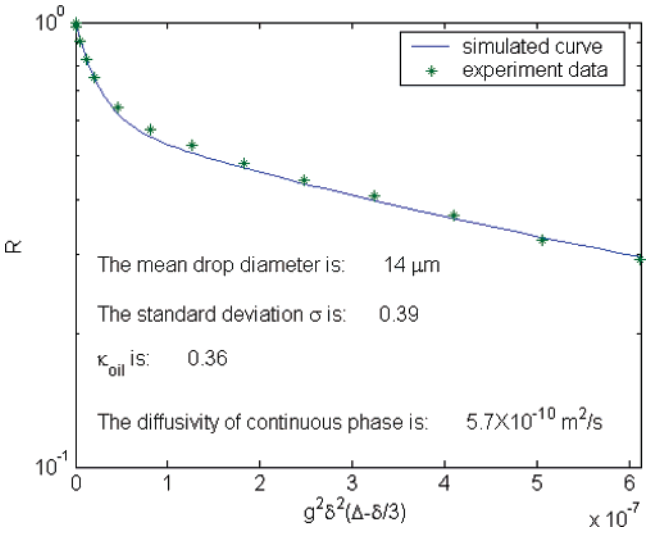

Figure 7. Fitting results of diffusion measurement for the emulsions (sample 1).

Table 3. Calculation Results of Emulsion with Solids and No PR_5 (Sample 1)

age (h)	mean diameter (m)	σ	κ_{oil}	κ_{water}	κ_{emul}
0.8	15	0.40	0.37	0.02	0.61
1.6	14	0.39	0.36	0.02	0.62
3.2	12	0.41	0.39	0.04	0.57
4.8	12	0.42	0.39	0.04	0.57
5.6	12	0.41	0.39	0.04	0.57
8.0	12	0.40	0.40	0.05	0.55
11.2	11	0.42	0.41	0.05	0.54

middle of the sample. The latter ranges from −2 cm to 2 cm, so the total length is 4 cm, which is equal to the height of the sample.

The T_1 value of water is greater than that of diluted bitumen, so the amplitude of water is smaller than that for diluted bitumen, based on eq 2. Thus, in the profile results, the signal amplitude of water is smaller than that of oil. Based on the T_1 difference, the signal amplitudes of different phases in the emulsion become distinguishable.

Table 4. Calculation Results of Emulsion with Solids and Added PR_5 (Sample 2)

age (h)	mean diameter (μm)	σ	κ_{oil}	κ_{water}	κ_{emul}
0.8	17	0.50	0.49	0.05	0.51
1.6	13	0.50	0.50	0.10	0.40
3.2	14	0.52	0.44	0.13	0.43
4.8	12	0.53	0.45	0.16	0.39
5.6	11	0.70	0.41	0.23	0.33
8.0	11	0.72	0.38	0.29	0.33
11.2	11	0.62	0.40	0.30	0.30

Table 5. Calculation Results of Emulsion without Solids and No PR_5 (Sample 3)

age (h)	mean diameter (μm)	σ	κ_{oil}	κ_{water}	κ_{emul}
0.8	11	0.33	0.31	0	0.69
1.6	11	0.33	0.31	0	0.69
3.2	11	0.34	0.32	0	0.68
4.8	11	0.35	0.34	0	0.66
5.6	11	0.35	0.33	0	0.67
8.0	12	0.36	0.33	0	0.67
11.2	12	0.36	0.32	0	0.68

Table 6. Calculation Results of Emulsion without Solids and Added PR_5 (Sample 4)

age (h)	mean diameter (μm)	σ	κ_{oil}	κ_{water}	κ_{emul}
0.8	20	0.70	0.54	0.30	0.16
1.6	23	0.64	0.20	0.68	0.12
3.2	27	0.57	0.20	0.70	0.10

A comparison of samples 1 and 3 with samples 2 and 4 shows that coalescence is much more significant with added PR_5, which shows that PR_5 can accelerate emulsion coalescence. A comparison of samples 2 and 4 shows that the solids in sample 2 prohibit complete separation and form a middle rag layer, which is the focus of further studies.

If profile measurements are performed over time, the evolution of the emulsion (such as sedimentation and coalescence) can be obtained from the results. The water fraction profile can be obtained from the profile results if some simple assumptions are valid:

(1) T_1 for the oil, water droplet, and bulk water can be considered as distinct single values, rather than a distribution. Thus, eq 3 can be used for water fraction calculation.

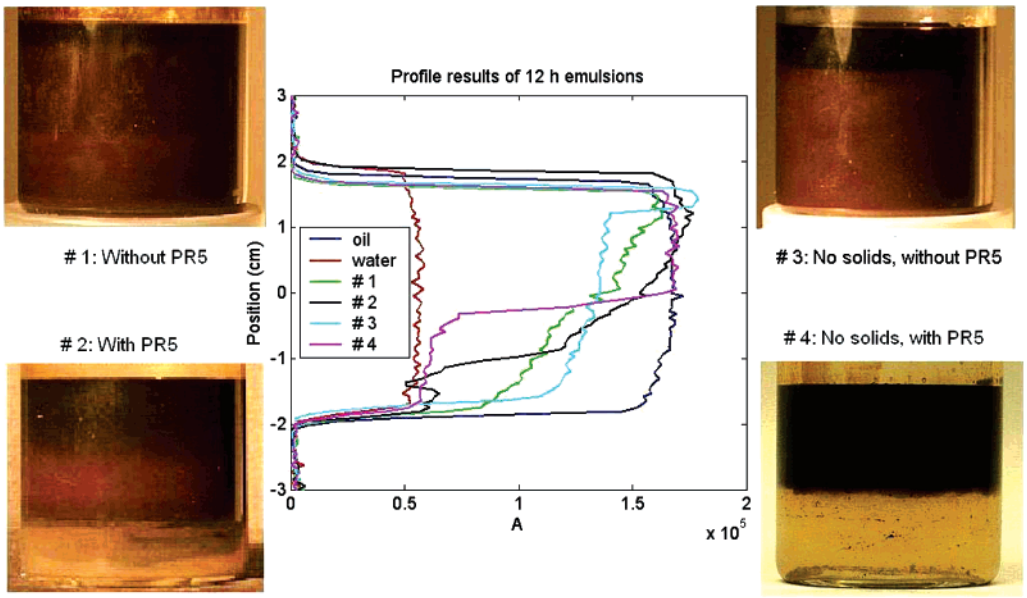

Figure 8. Profile measurement results of emulsion samples.

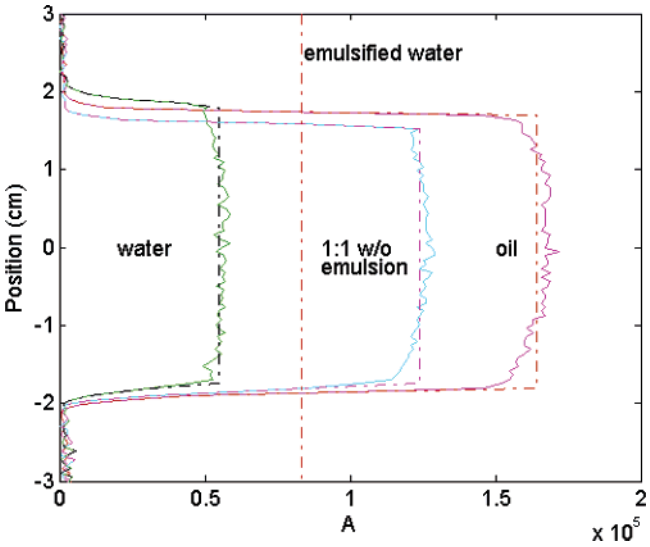

Figure 9. Calibration for calculation of water fraction (sample 1).

(2) The changes in T_1 during the experimental time can be ignored. Thus, the experimental data for fresh homogeneous emulsion can be used to calibrate for later times.

(3) In the samples without PR_5, emulsion coalescence is insignificant. These samples contain only W/O emulsion. In the samples with PR_5, emulsified water coexists with either clean oil or free water, but not both. On the top is clean oil and emulsified water; at the bottom is a water-in-oil-in-water (W/O/W) emulsion and free water.

The calculation process is shown in Figure 9 for sample 1. First, the water amplitude (A_w), a $T_{1,w}$ value of 2.6 s, and eq 8 are used to calculate A_∞:

$$A_w = A_\infty\left[-\exp\left(\frac{-t_w}{T_{1,w}}\right)\right] \Rightarrow \text{calculate } A_\infty \qquad (8)$$

The oil amplitude (A_o) and eq 9 are used to calculate T_{1o} for oil:

$$A_o = A_\infty\left[1 - \exp\left(\frac{-t_w}{T_{1o}}\right)\right] \Rightarrow \text{calculate } T_{1o} \qquad (9)$$

The fresh homogeneous emulsion amplitude (A_{emul}) and eq 10 are used to calculate $T_{1,emul}$ for emulsified water:

$$A_{emul} = A_\infty\left[1 - \Phi_{emul}\exp\left(\frac{-t_w}{T_{1,emul}}\right) - (1 - \Phi_{emul})\exp\left(\frac{-t_w}{T_{1o}}\right)\right] \Rightarrow \text{calculate } T_{1,emul} \qquad (10)$$

In Figure 9, the red dash-dotted line is the calculated amplitude value of emulsified water from calibration. This is the lower bound of the amplitude for the system. Similarly, the pure oil amplitude is the upper bound of the amplitude for the system. Values below or above these bounds can be considered as fully saturated water or clean oil, respectively.

The parameters A_∞, $T_{1,w}$, $T_{1,o}$, and $T_{1,emul}$ are known from calibration. T_1 values, emulsion data for A_{emul}, and eq 3 can be used to calculate the water fraction. Equation 3 can be simplified as follows:

$$A_{emul}(z) = A_\infty\left[1 - \varphi_{oil}(z)\exp\left(\frac{-t_w}{T_{1,oil}}\right) - \varphi_{drop}(z)\exp\left(\frac{-t_w}{T_{1,drop}}\right)\right] \qquad (11a)$$

$$\varphi_{oil}(z) + \varphi_{drop}(z) = 1 \qquad (11b)$$

$$A_{emul}(z) = A_\infty\left[1 - \varphi_{water}(z)\exp\left(\frac{-t_w}{T_{1,water}}\right) - \varphi_{drop}(z)\exp\left(\frac{-t_w}{T_{1,drop}}\right)\right] \qquad (12a)$$

$$\varphi_{water}(z) + \varphi_{drop}(z) = 1 \qquad (12b)$$

In eqs 11 and 12, A_{emul}, A_∞, t_w, and T_1 values are known. The component fractions φ can be calculated from the equation.

As indicated previously, the samples without PR_5 contain only oil and emulsified water drops. Equation 11 can be used to calculate water fraction.

In the samples with PR_5, emulsified water coexists with clean oil at the top. Equation 11 can be used to calculate the emulsified water fraction. At the bottom is a W/O/W emulsion and free water, and eq 12 can be used to calculate the free-water fraction.

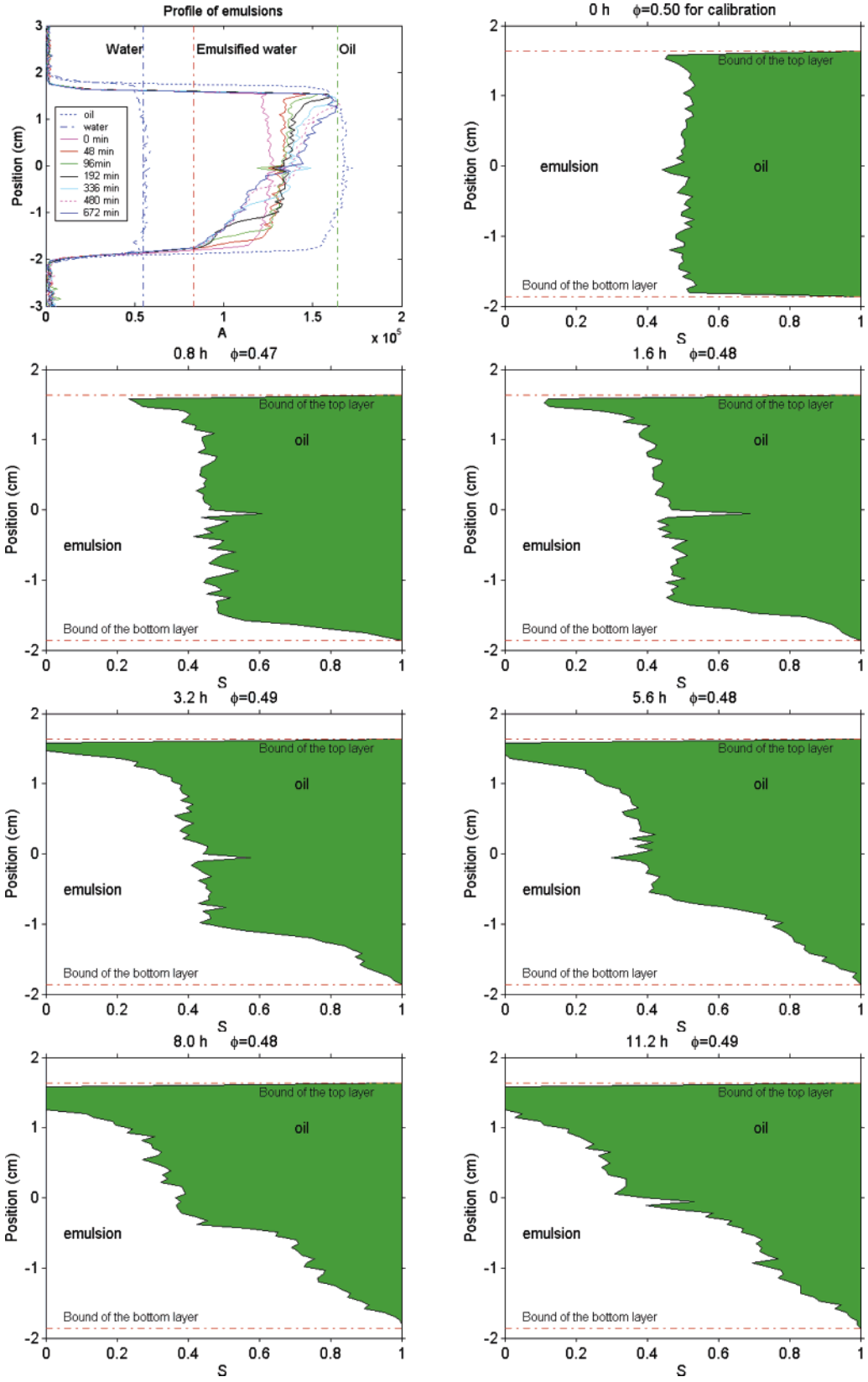

Figure 10. Profile results and water fractions of sample 1 (with solids, no PR_5).

The profile results and calculated water fraction profiles of samples 1−4 are shown in Figures 10−13. The red dashed lines in the figures represent the boundaries of the sample. The total height is slightly less than 4 cm. The *x*-axis represents the emulsified or free-water saturation of the sample (*S*), and the *y*-axis position is the position measured from the middle of the sample.

The waiting time is $t_w = 0.6$ s. The total water content (0.50) is used for calibration in the first figure. For other water-fraction profile figures at later times, the total water content (Φ) obtained

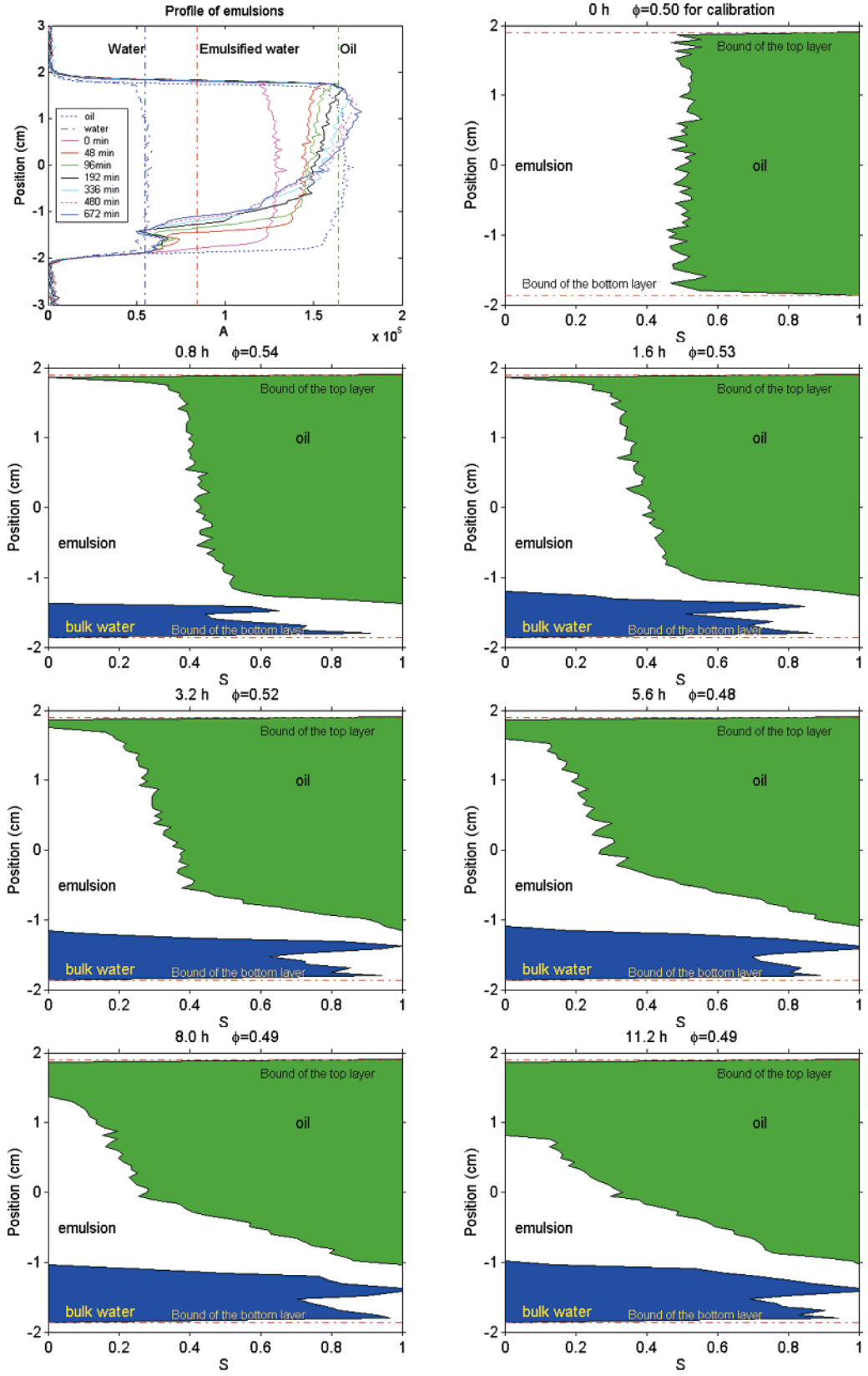

Figure 11. Profile results and water fractions of sample 2 (with solids and added PR_5).

by integration over the vertical position is listed, to demonstrate consistency. For all four samples, the calculated and actual water contents were almost equal at all times.

In the calculation of sample 1 (with solids, no PR_5; see Figure 10), the T_1 values for bulk water, oil, and emulsified water are 2.60, 0.63, and 1.41 s, respectively. The first two of these, being bulk-phase properties, are the same for all four samples. At the initial time, the emulsion is homogeneous, and the water fraction is ~0.5. As the time increases, the dispersed water fraction increases at the bottom and decreases on the top. This result is consistent with the visual observation of emulsion sedimentation.

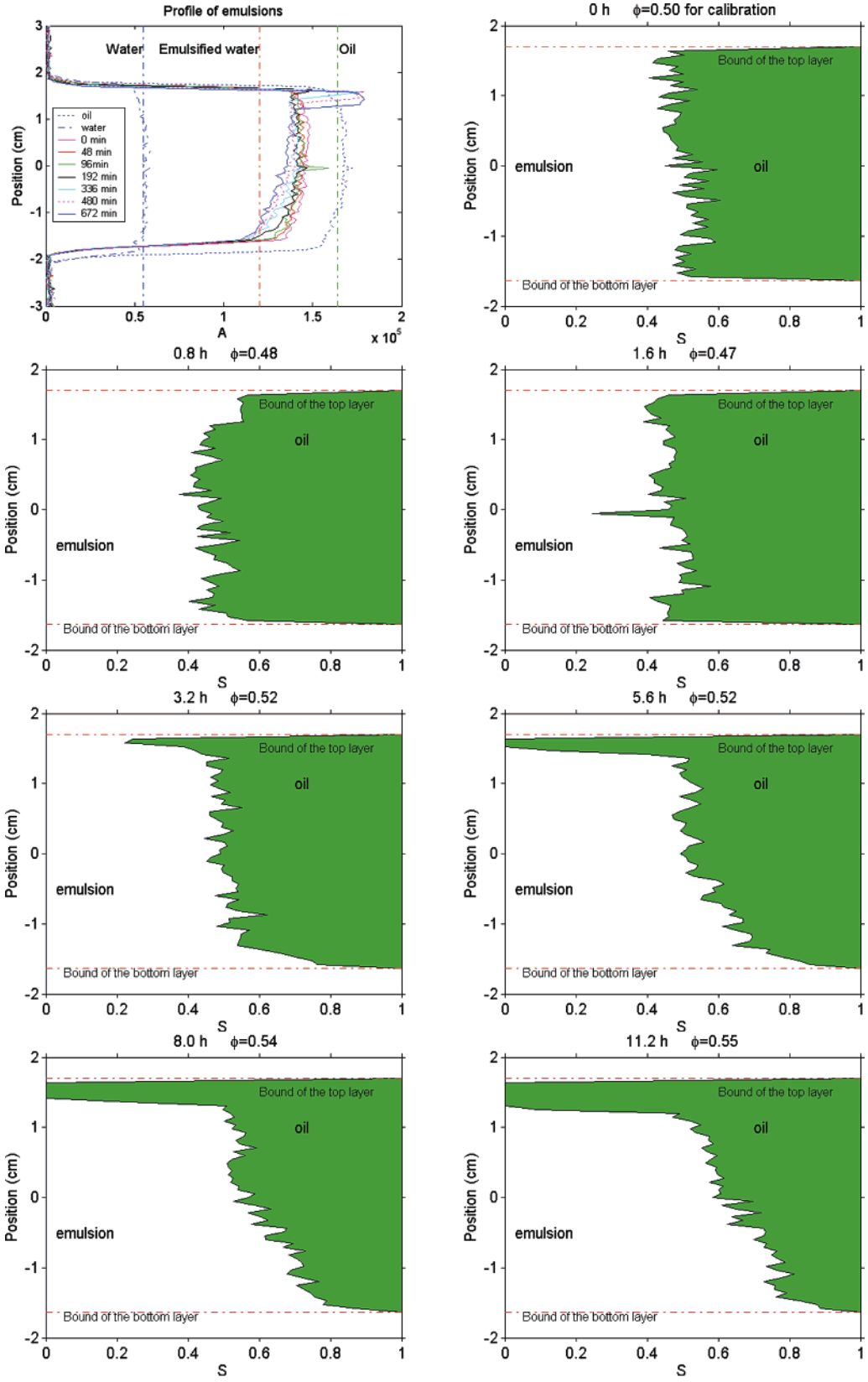

Figure 12. Profile results and water fractions of sample 3 (without solids or PR_5).

From water-fraction profiles, it is easy to see that the sample has three layers. On the top, the water fraction is zero, which corresponds to a clean oil layer. In the middle, the water fraction is ~0.5, which corresponds to a W/O emulsion layer. At the bottom, water fraction is between 0.5 and 1.0, which corresponds to a concentrated W/O emulsion layer. The step change of the water fraction corresponds to the front between two layers.

In the calculation of sample 2 (with solids and PR_5; see Figure 11), the T_1 values for the bulk water, oil, and emulsified water

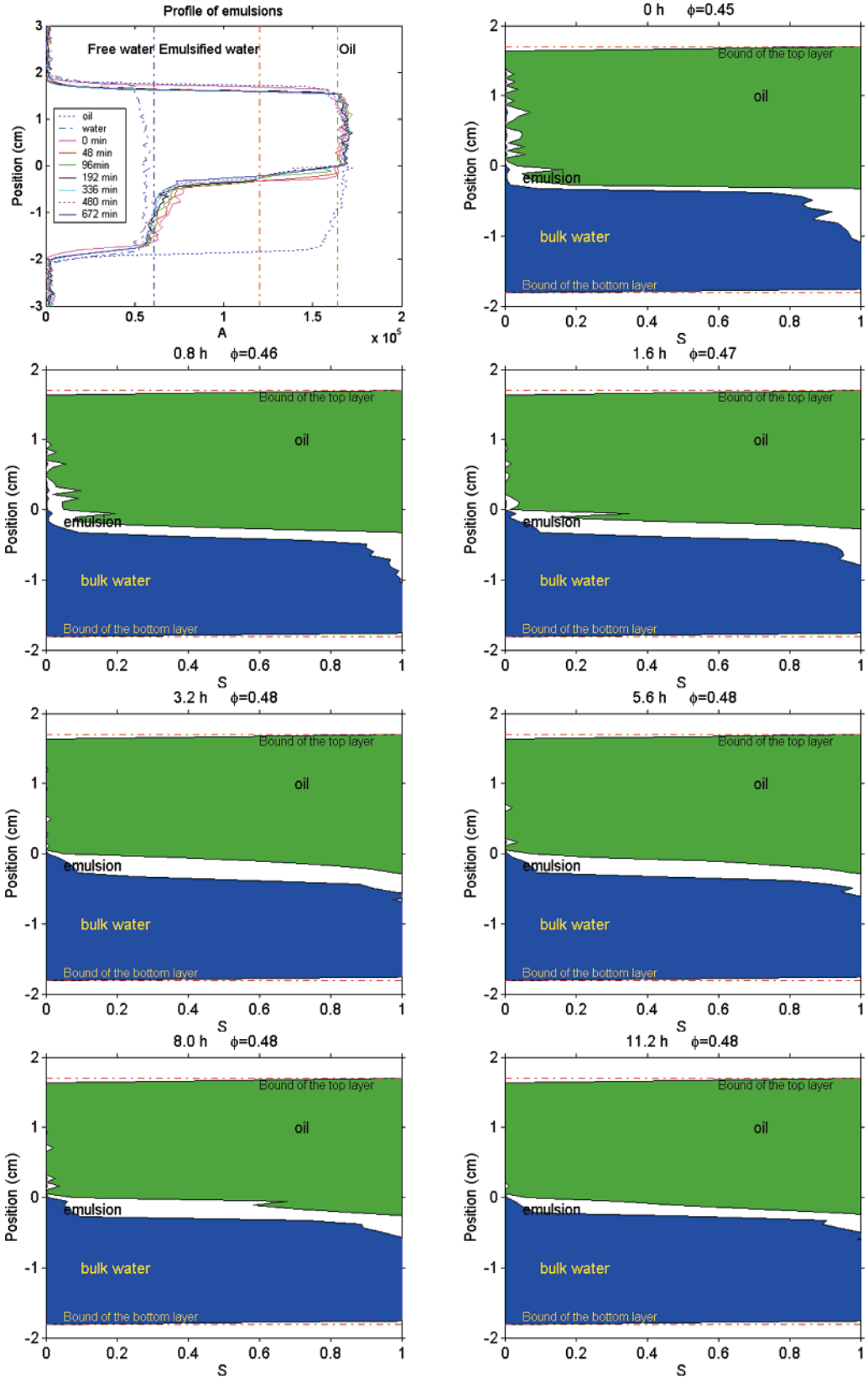

Figure 13. Profile results and water fractions of sample 4 (without solids, with added PR_5).

are 2.60, 0.63, and 1.46 s, respectively. Besides the sedimentation, coalescence occurs at the same time.

The sample with PR_5 can achieve more-complete separation than that without PR_5. Hence, on the top, the signal amplitude is similar to that of pure oil, and at the bottom, the signal amplitude is similar to that of bulk water. These results correspond to the results in Figure 8, which shows that the top is pure oil, the middle is an emulsion layer, and the bottom is mostly separated free water. The emulsified water T_1 values of samples 1 and 2 are very similar, which shows consistency of

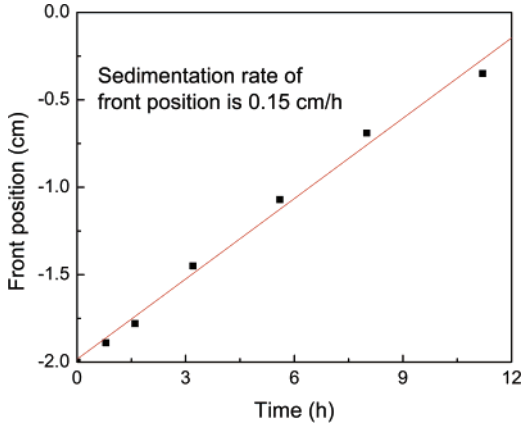

Figure 14. Front position and sedimentation rate of emulsion sample 1.

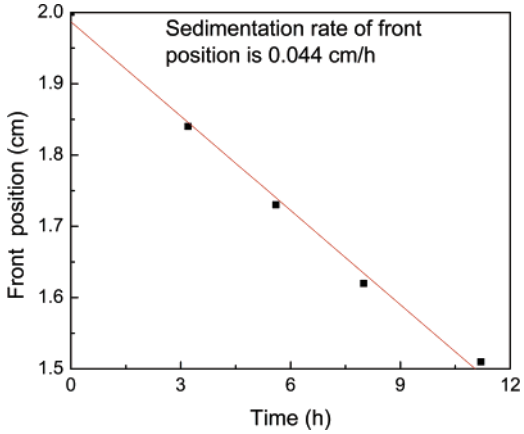

Figure 15. Front position and sedimentation rate of emulsion sample 3.

the mixing process with given oil and water phases and indicates that the small amount of demulsifier in sample 2 does not significantly affect emulsified water T_1 values.

In the calculation of sample 3 (no solids, no PR_5; see Figure 12), the T_1 values for the bulk water, oil, and emulsified water are 2.60, 0.63, and 1.11 s, respectively. The results of sample 3 are similar to those of sample 1. On the top, the water fraction is zero, which corresponds to a clean oil layer. In the middle, the water fraction is ~0.5, which corresponds to a W/O emulsion layer. At the bottom, the water fraction is ~1.0, which corresponds to a concentrated W/O emulsion layer.

In the calculation of sample 4 (no solids, with PR_5; see Figure 13), the T_1 values for the bulk water, oil, emulsified water, and separated free water are 2.60, 0.63, 1.11, and 2.32 s, respectively. Here, the T_1 value for emulsified water cannot be obtained from the calibration of sample 4, because, at the initial time, sample 4 is not homogeneous, because of rapid coalescence. Thus, here, the T_1 value for emulsified water is assumed to be that obtained from the calibration of sample 3. The T_1 value for separated free water (2.10 s) is also shorter than that of pure bulk water and is obtained from a separate NMR measurement.

For sample 4, from water-fraction profiles, the separation of oil and water is complete. On the top, the water fraction is close to zero, which corresponds to a clean oil layer. At the bottom, the water fraction is 1.0, which corresponds to free water.

3.4. Sedimentation Rate from 1-D T_1 Weighted Profile Measurement. In the profile results of samples 1 and 3, the step change in signal amplitude is a response to the sedimentation front (boundary between different layers). Hence, the velocity of the front can be obtained from profile measurement results. As a result of sedimentation of the water droplets, the clean oil layer resides at the top of the sample, the emulsion layer resides in the middle, and the concentrated emulsion layer resides at the bottom.

Figure 14 shows the position of the sedimentation front between the concentrated emulsion layer and the emulsion layer of sample 1 (with solids and no PR_5), as a function of time. At time zero, the sedimentation front starts from the bottom of the sample (−2 cm in Figure 10), and it moves upward with time. The front velocity (dh/dt) can be calculated by fitting the experimental data.

If we assume that the water fraction in each layer does not change during sedimentation, the sedimentation velocity within the emulsion can be obtained by applying a mass balance across the sedimentation front. If there is negligible sedimentation in the concentrated emulsion with volume fraction φ_{max}, the sedimentation velocity of water droplets in the emulsion above the front is given by

$$v_{lower} = \frac{\varphi_{max} - \varphi_e}{\varphi_e}\frac{dh}{dt} \qquad \text{(lower front)} \qquad (13)$$

In sample 3 (no solids, no PR_5; see Figure 12), a sharp front moving upward from the bottom is less evident. However, a front moving downward from the top of sample 3 (although less clearly in sample 1) can be seen with almost water-free oil above and emulsion below (Figure 15). A similar mass balance yields

$$v_{upper} = \frac{\varphi_{min} - \varphi_e}{\varphi_e}\frac{dh}{dt} = -\frac{dh}{dt} \qquad \text{(upper front)} \qquad (14)$$

In these equations, h is the front position, v_{lower} and v_{upper} are the sedimentation velocity of water droplets in the emulsion, whose volume fraction φ_e is assumed to be 0.50. The average water fraction in the concentrated emulsion layer (0.75) can be used as the φ_{max} value, and the average water fraction in the clean oil layer φ_{min} is close to zero.

The predicted sedimentation velocity of the emulsion can be calculated with the following equation, which is an empirical modification of Stokes' Law:[4]

$$v = \frac{\Delta\rho g d^2}{18\eta_C}(1 - \varphi_e)^n \qquad (15)$$

Here, φ_e is again 0.50 and n is 8.6. $\Delta\rho$ (refer to Table 1) is the density difference between the water and the oil, g the gravitational acceleration, d the mean diameter of water droplets, and η_C the viscosity of the oil phase.

The experimental sedimentation velocity of water droplets for sample 1 with eq 13 is 0.075 cm/h, whereas the predicted value from eq 15 is 0.0105 cm/h. The larger experimental value implies that the water drops sediment with a larger effective drop size. Therefore, the emulsion may be flocculated.

The same calculation procedure with eq 14 can be applied to the upper front of sample 3, using the data of Figure 15. Here, φ_e is 0.50. The experimental sedimentation velocity of water droplets is 0.044 cm/h, whereas the predicted value is 0.0103 cm/h. Their ratio is ~4:1, which indicates that some

(4) Richardson, J. F.; Zaki, W. N. Sedimentation and Fluidisation: Part I. *Trans. Inst. Chem. Eng.* **1954**, *32*, 35−53.

flocculation likely also occurs in this case. However, further investigation of flocculation in these emulsions is desirable.

4. Conclusions

Stable water in diluted bitumen emulsions persist in the absence of a coalescer at room temperature. The coalescence rate of the emulsion is very slow and is difficult to observe, even if most of the clay solids are removed by centrifuge before the emulsion preparation. The sedimentation rate is much faster, compared with coalescence. Solids in the emulsion sample can promote flocculation and increase the rate of sedimentation.

PR_5 is an optimal coalescer for the brine in diluted bitumen emulsions at room temperature. For emulsion samples with or without solids, PR_5 can accelerate the coalescence rate. For the sample without solids, complete separation can be obtained; for the sample with solids, a rag layer, which contains solids and has intermediate density, forms between the clean-oil and free-water layers. This rag layer prevents further coalescence and complete separation of the emulsified water.

A novel approach to process experimental data from classic nuclear magnetic resonance (NMR) experiments for the characterization of water-in-oil (W/O) emulsions has been proposed and tested in emulsions of water in diluted bitumen. Carr−Purcell−Meiboom−Gill (CPMG) NMR analysis methods can be used to measure the T_2 distribution of W/O emulsions. However, in the emulsion sample with solids and no PR_5, the T_2 distributions of the dispersed water phase and the continuous oil phase are not distinguishable, with the result that the drop-size distribution of the emulsion cannot be obtained from CPMG measurement. In this case, NMR restricted diffusion experiment (pulsed gradient spin−echo (PGSE)) can be used to measure the emulsion drop-size distribution. Experimental data for the samples without PR_5 from PGSE measurements show that the emulsion drop size and the attenuation factor κ for each component do not change much with time, which is consistent with the observation that these emulsions are very stable without the coalescer. After adding PR_5, κ for emulsified water decreases and κ for free water increases, which implies coalescence of the emulsion.

NMR one-dimensional (1-D) T_1 weighted profile measurement can distinguish the composition variation of the sample in the vertical direction. The sedimentation rate of the front position and water droplet sedimentation velocity can be obtained from profile results. Emulsion flocculation can be deduced by comparing the sedimentation velocity from experimental data and modified Stokes' Law predictions. Free-water- and dispersed-water-fraction profiles can be obtained from the profile results, using pure water and oil as the reference. Coalescence can be detected from the time evolution of the free-water fraction profile.

EF0604487